Electronic Supplementary Material (ESI) for Inorganic Chemistry Frontiers.
This journal is © the Partner Organisations 2019

Supporting Information

Effective Removal of Uranium from Aqueous Solution by Using Novel Sustainable Porous Al_2O_3 Materials Derived from Different Precursors of Aluminum

Jun Liao[a,b], Yong Zhang[a,b *]

[a] State Key Laboratory of Environmental Friendly Energy Materials, School of National Defence Science and Technology, Southwest University of Science and Technology, Mianyang 621010, P. R. China

[b] Sichuan Co-Innovation Center for New Energetic Materials, Southwest University of Science and Technology, Mianyang 621010, P. R. China

[*]Corresponding author. E-mail: pandmzy@foxmail.com (Y. Zhang).

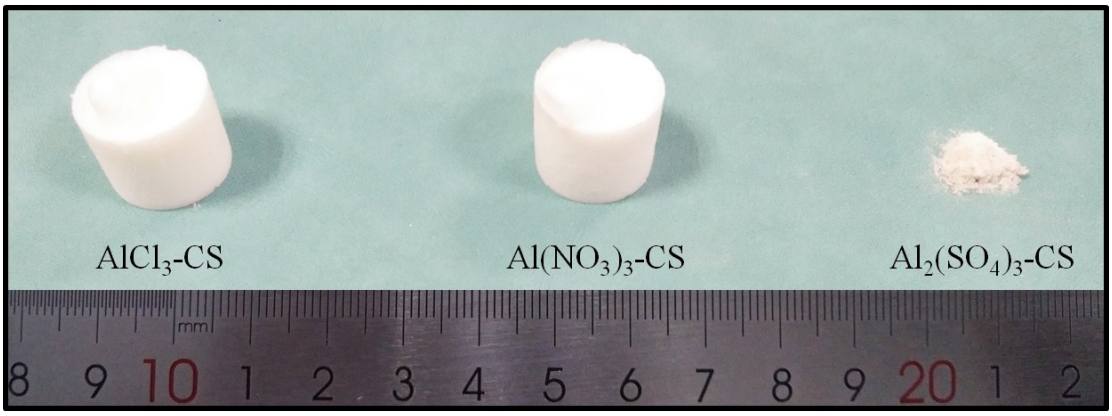

Figure S1. Photos of $AlCl_3$-CS, $Al(NO_3)_3$-CS and $Al_2(SO_4)_3$-CS composites.

Table S1. The density for the synthesis of $AlCl_3$-CS, $Al(NO_3)_3$-CS and $Al_2(SO_4)_3$-CS composites.

Samples	m(mg)	d(cm)	h(cm)	V(cm^3)	ρ(mg/cm^3)
$AlCl_3$-CS	94.32	2.30	2.30	9.55	9.88
$Al(NO_3)_3$-CS	96.77	2.25	2.30	9.15	10.58
$Al_2(SO_4)_3$-CS	–	–	–	–	–

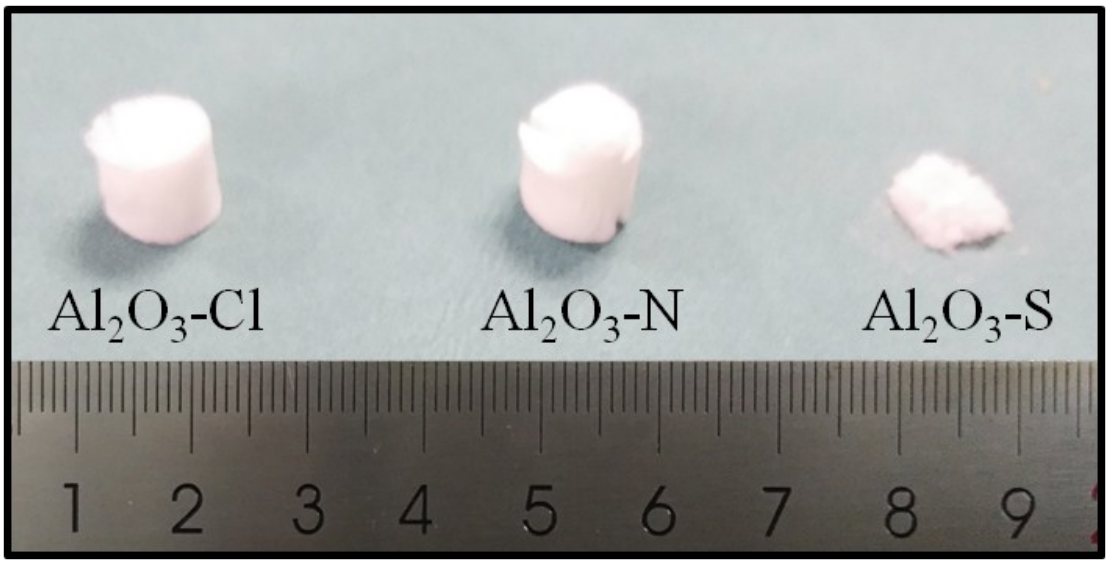

Figure S2. Photos of porous Al_2O_3-Cl, Al_2O_3-N and Al_2O_3-S materials.

Table S2. The density for the synthesis of porous Al_2O_3-Cl, Al_2O_3-N and Al_2O_3-S materials.

Samples	*m* (mg)	*d* (cm)	*h* (cm)	*V* (cm^3)	ρ (mg/cm^3)
Al_2O_3-Cl	6.93	1.10	1.10	1.05	6.60
Al_2O_3-N	7.71	1.05	1.10	0.95	8.12
Al_2O_3-S	–	–	–	–	–

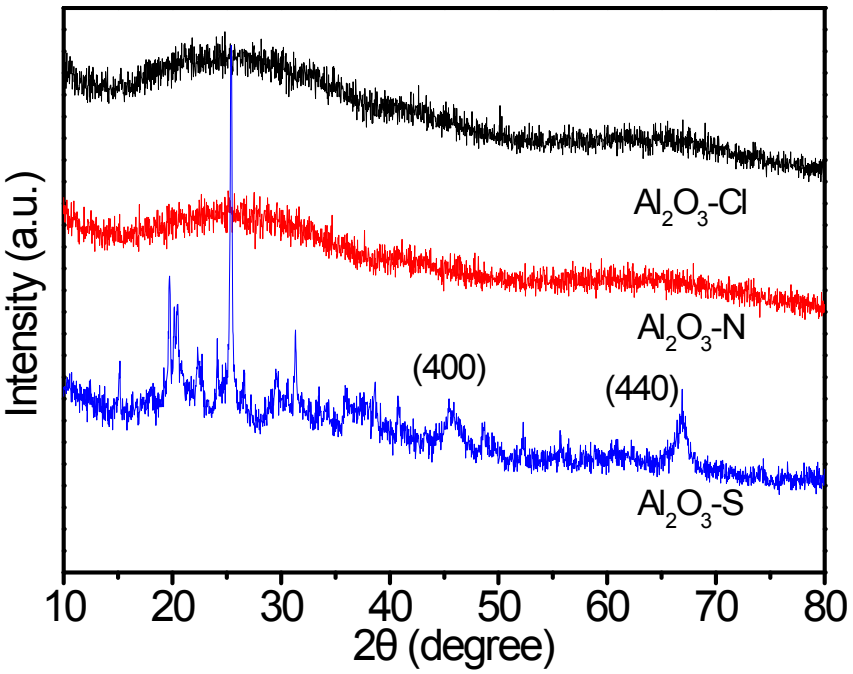

Figure S3. XRD patterns of porous Al_2O_3-Cl, Al_2O_3-N and Al_2O_3-S materials.

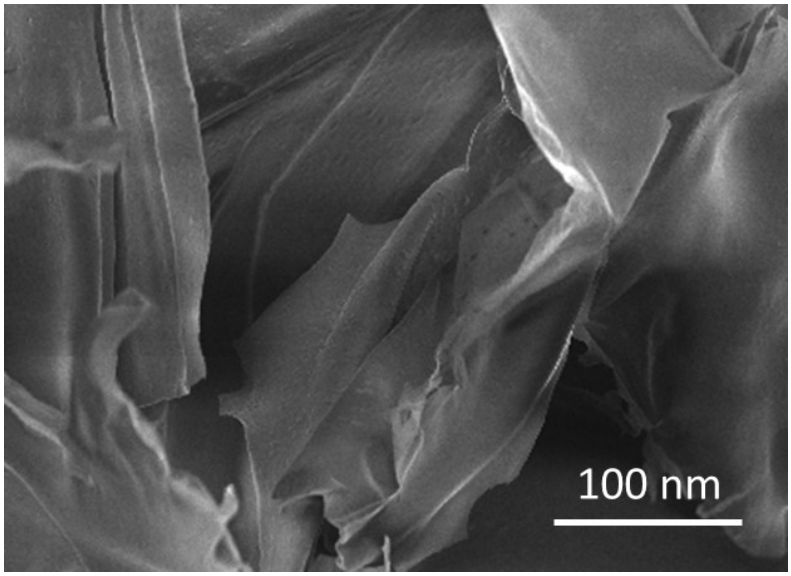

Figure S4. SEM image of pure chitosan viewed at high magnifications.

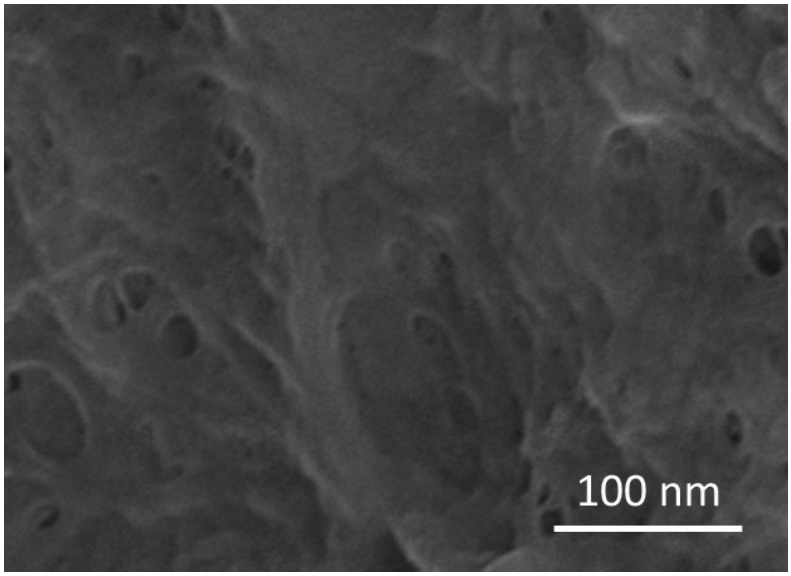

Figure S5. SEM image of $AlCl_3$-CS composite viewed at high magnifications.

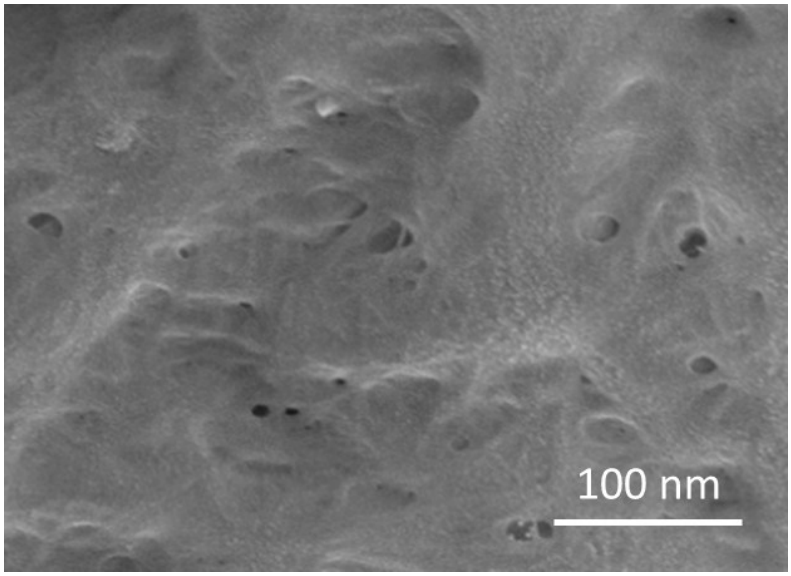

Figure S6. SEM image of $Al(NO_3)_3$-CS composite viewed at high magnifications.

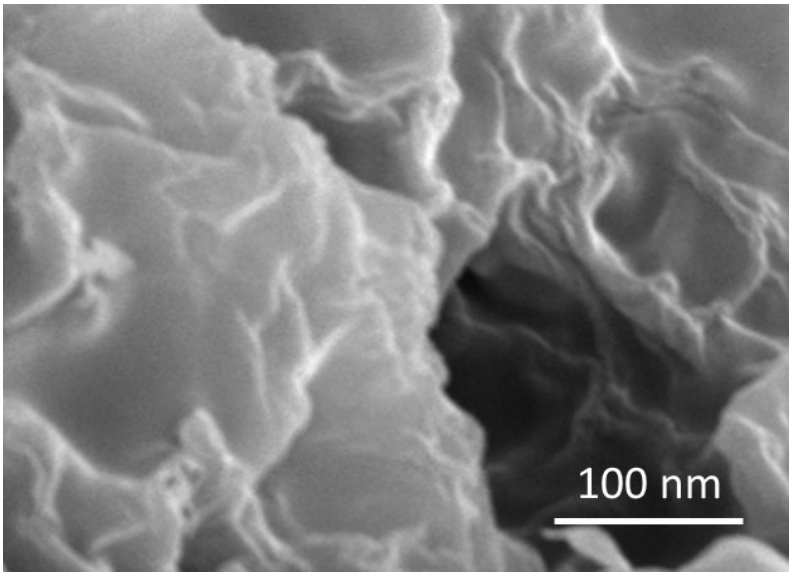

Figure S7. SEM image of $Al_2(SO_4)_3$-CS composite viewed at high magnifications.

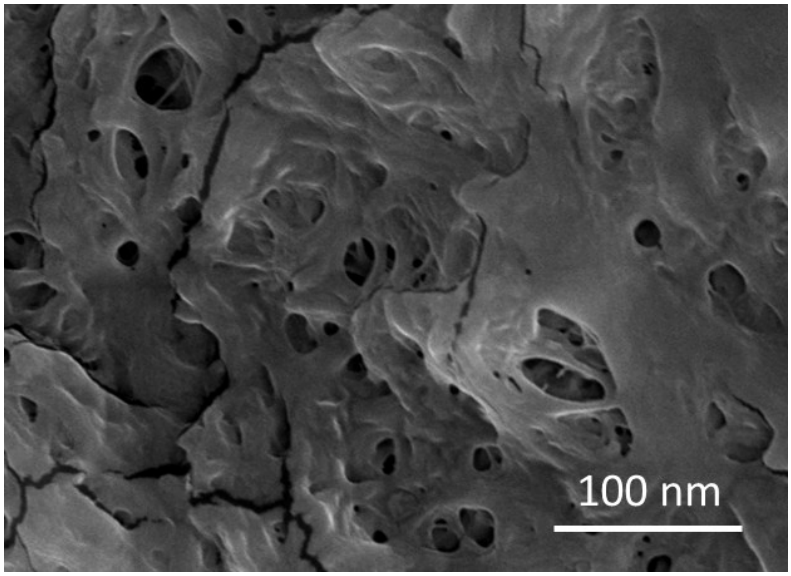

Figure S8. SEM image of Al_2O_3-Cl material viewed at high magnifications.

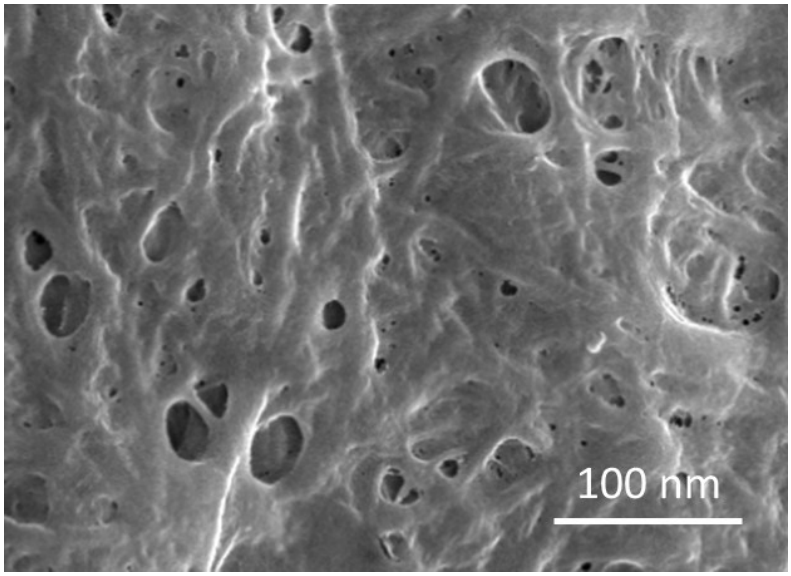

Figure S9. SEM image of Al_2O_3-N material viewed at high magnifications.

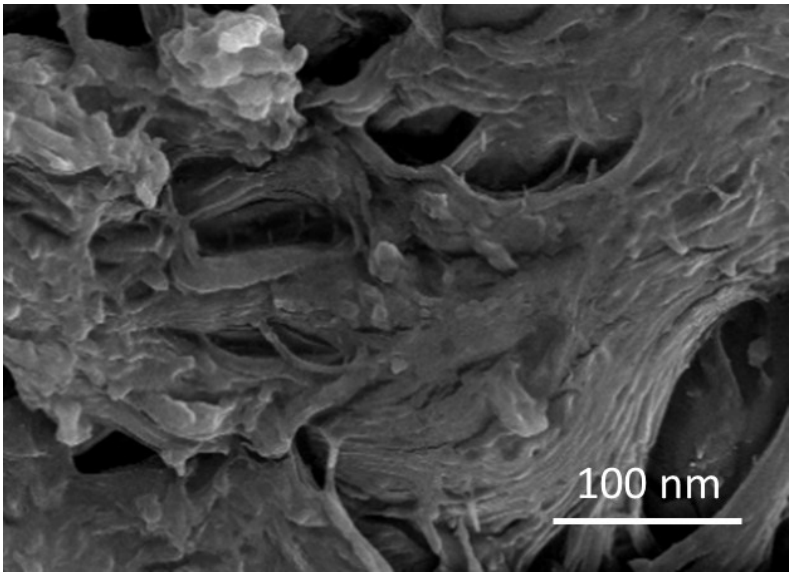

Figure S10. SEM image of Al_2O_3-S material viewed at high magnifications.

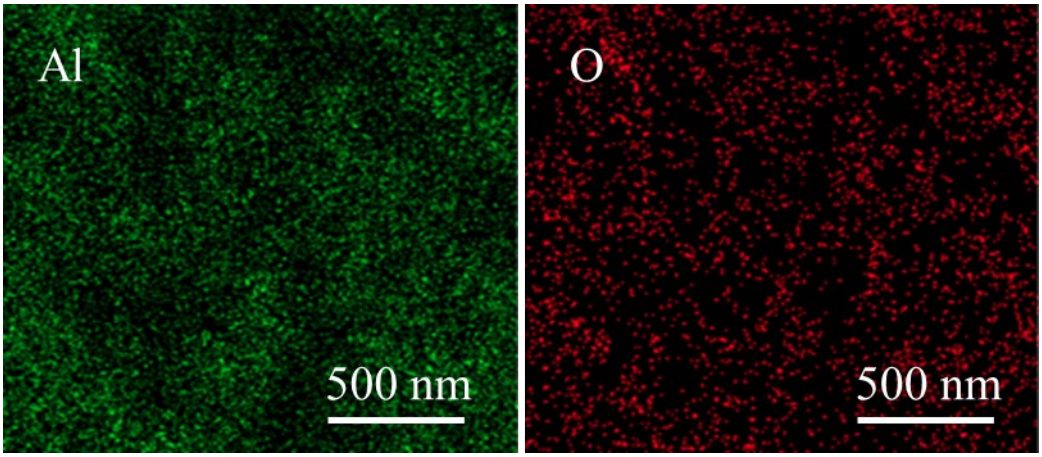

Figure S11. EDS mapping images of Al and O of Al_2O_3-Cl material.

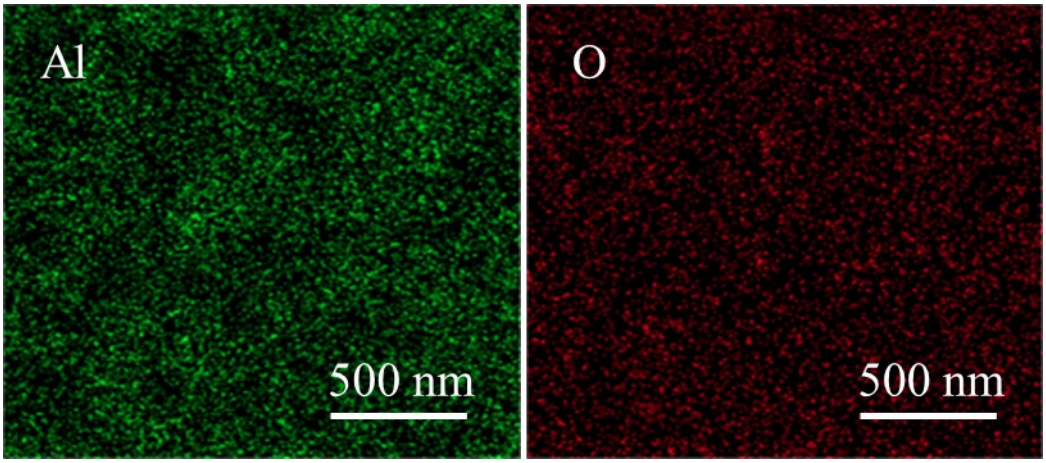

Figure S12. EDS mapping images of Al and O of Al_2O_3-N material.

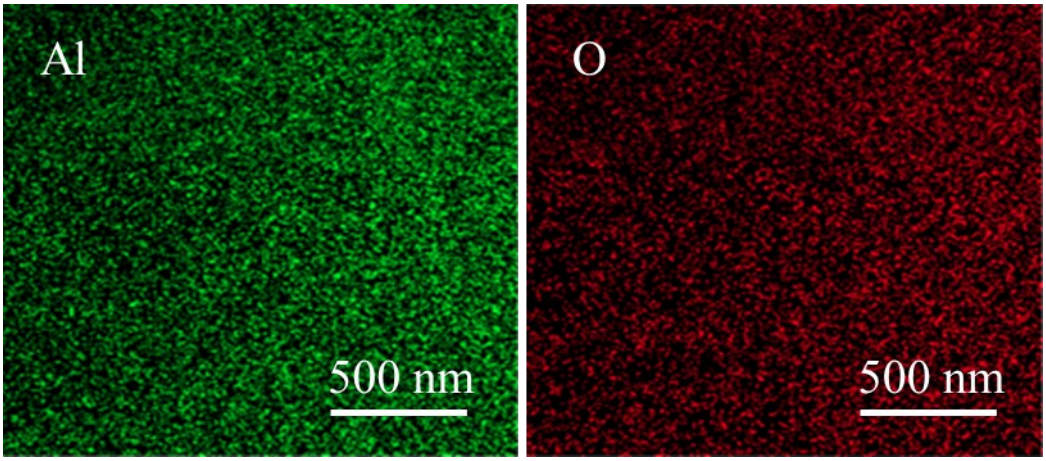

Figure S13. EDS mapping images of Al and O of Al_2O_3-S material.

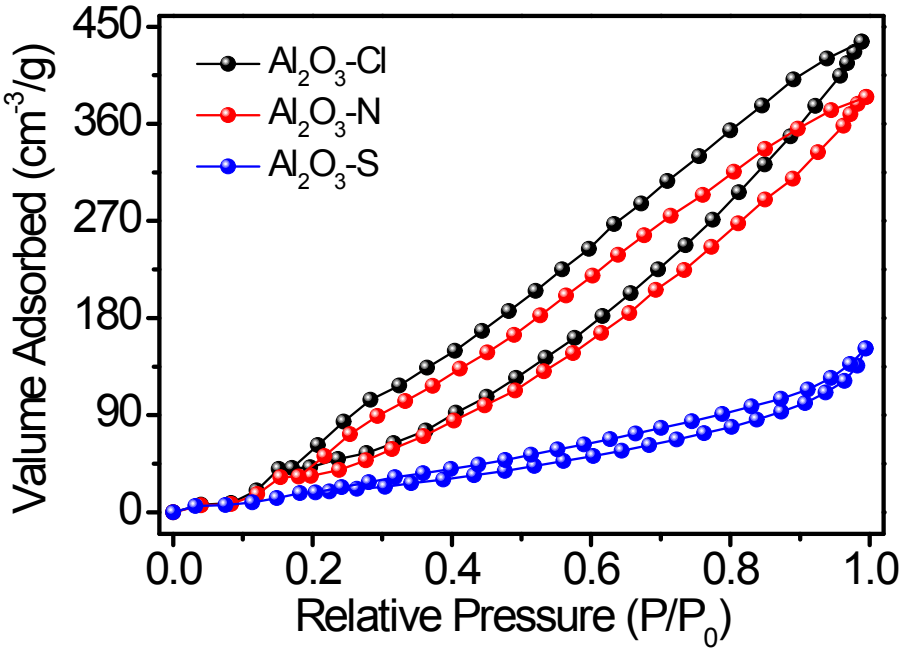

Figure S14. Nitrogen adsorption-desorption isotherms of porous Al_2O_3-Cl, Al_2O_3-N and Al_2O_3-S materials.

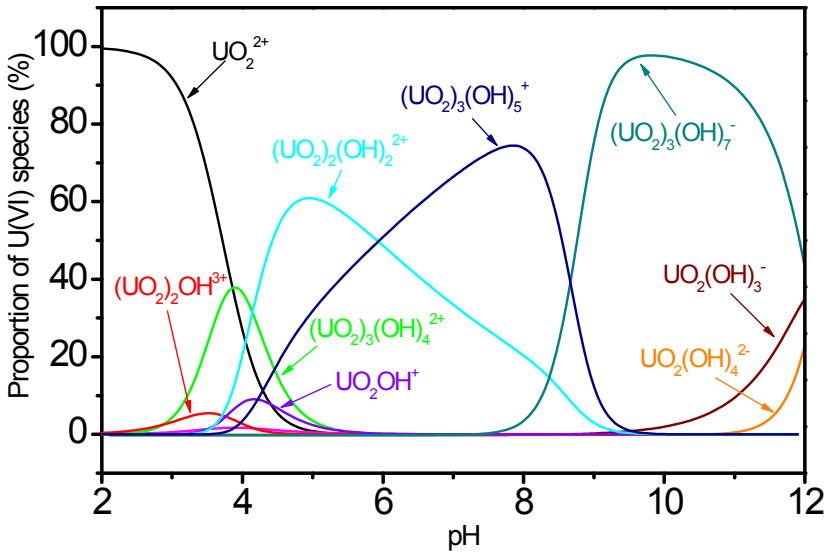

Figure S15. The distribution of U(Ⅵ) species in aqueous solution as a function of pH.

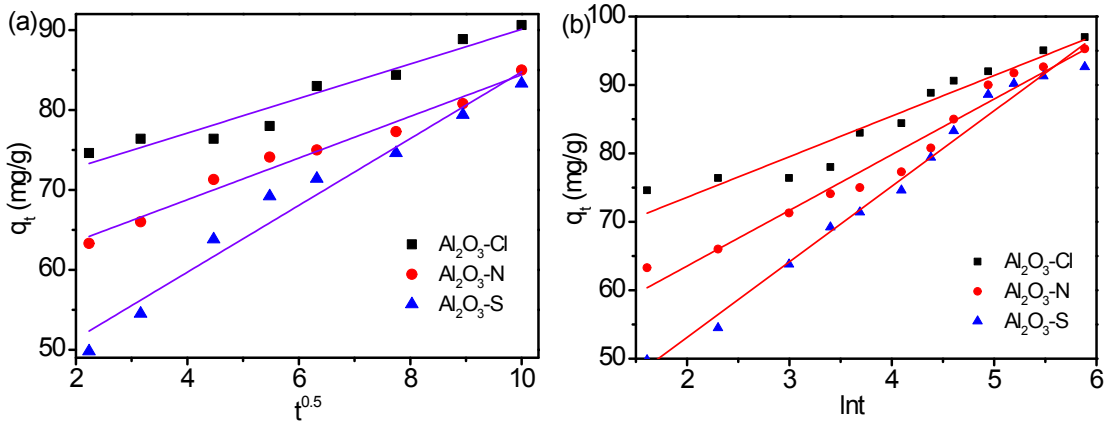

Figure S16. Linearized (a) intraparticle diffusion and (b) Elovich kinetic of U(VI) adsorption on porous Al_2O_3-Cl, Al_2O_3-N and Al_2O_3-S materials. T = 298 K, m/V = 0.1 g/L, $C_{initial}$ = 10.0 mg/L.

Table S4. Comparison of the maximum adsorption capacity of U(VI) by various adsorbents.

Adsorbents	T (K)	pH	Capacity (mg/g)	References
$Mg_3Si_4O_{10}(OH)_2$	298	7	41.6	[S1]
Fe_3O_4 NPs	298	6	95.2	[S2]
MSONs	298	4	526.6	[S3]
TNTs/$CoFe_2O_4$/TEPA	298	6	509.89	[S4]
ND-AO	298	4.5	212	[S5]
purchased Al_2O_3	298	6	10	[28]
Al_2O_3 nanofibers	298	5	204.1	[31]
Al_2O_3 microspheres	298	6	316.87	[32]
Al_2O_3-Cl	298	7	805.72	This work
Al_2O_3-N	298	7	716.74	This work
Al_2O_3-S	298	7	454.14	This work

Table S5. Comparison of the adsorption efficiency of U(VI) on metal oxide aerogels and other reported adsorbents.

materials	Adsorption efficiency		References
	distilled water (%)	seawater (%)	
poly(imide dioxime)	-	29	[S6]
Al_2O_3 microspheres	71.4	28.0	[32]
PO_4/PAO	77.6	36	[S7]
Al_2O_3-Cl	95.40	57.84	This work
Al_2O_3-N	92.99	53.33	This work
Al_2O_3-S	89.98	50.16	This work

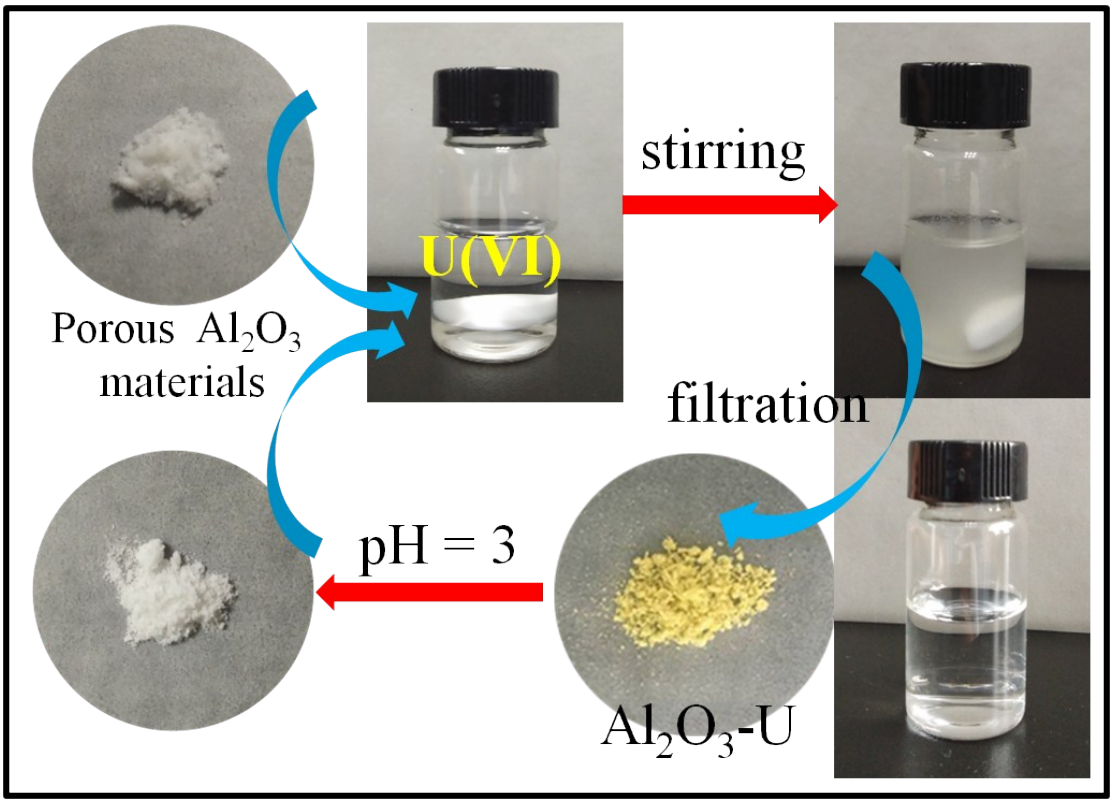

Figure S17. Chemical strategy for recycling of the porous Al_2O_3 materials in U(VI) adsorption.

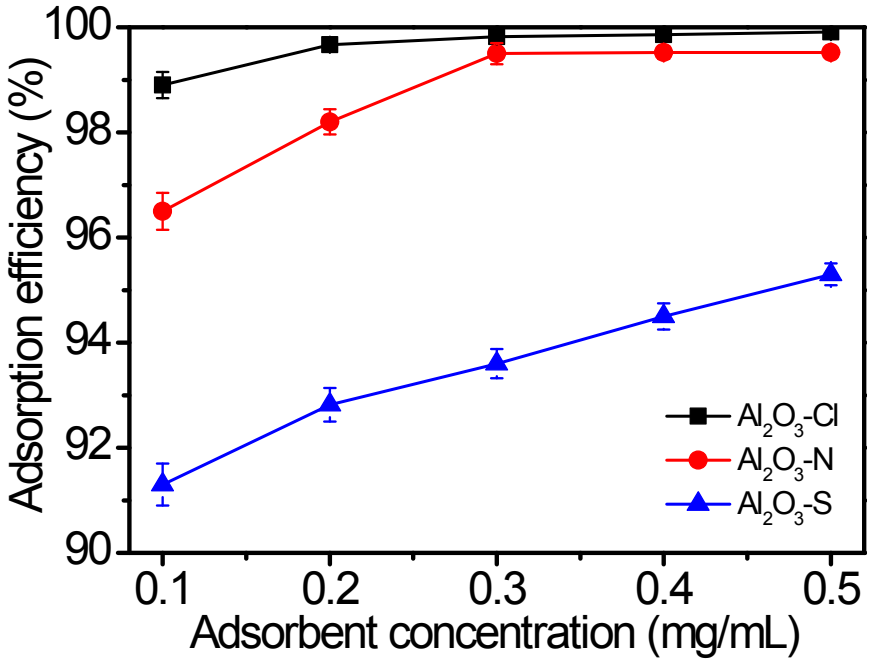

Figure S18. Effect of adsorbent amount on the adsorption efficiency of porous Al_2O_3-Cl, Al_2O_3-N and Al_2O_3-S materials, T = 298 K, pH = 7, $C_{initial}$ = 5.0 mg/L.

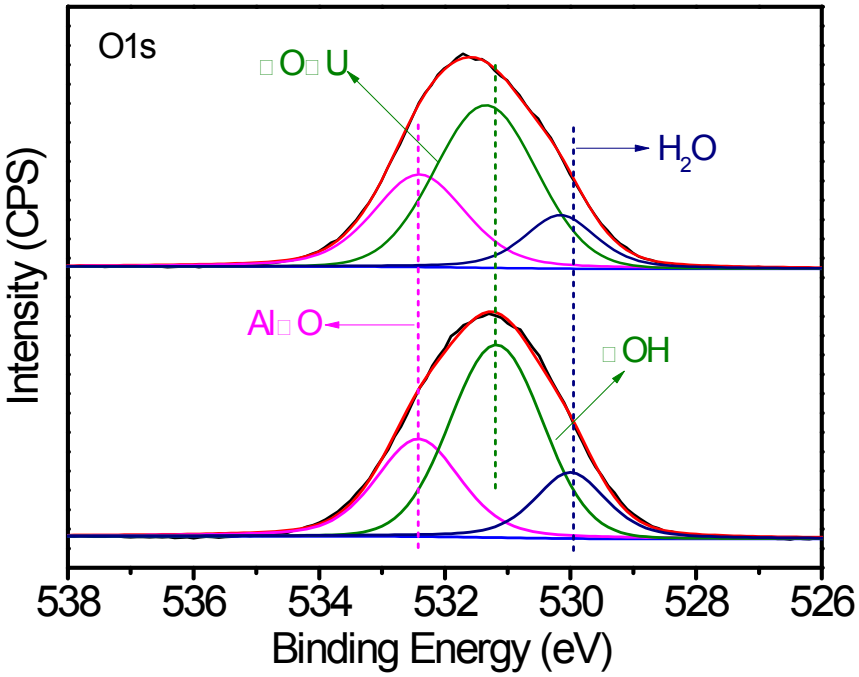

Figure S19. XPS high-resolution spectra of O1s for Al_2O_3-Cl before and after U(VI) adsorption.

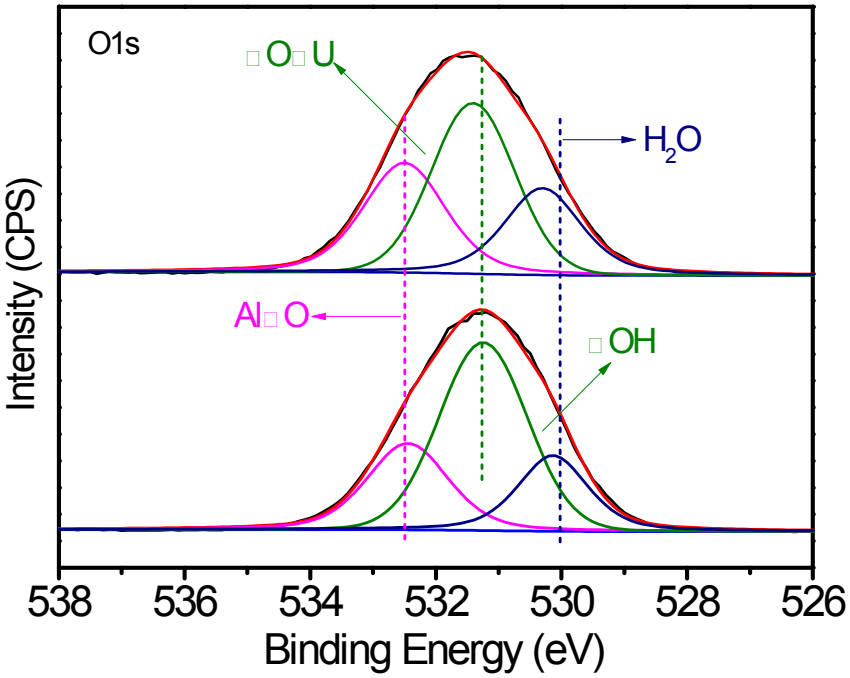

Figure S20. XPS high-resolution spectra of O1s for Al_2O_3-N before and after U(VI) adsorption.

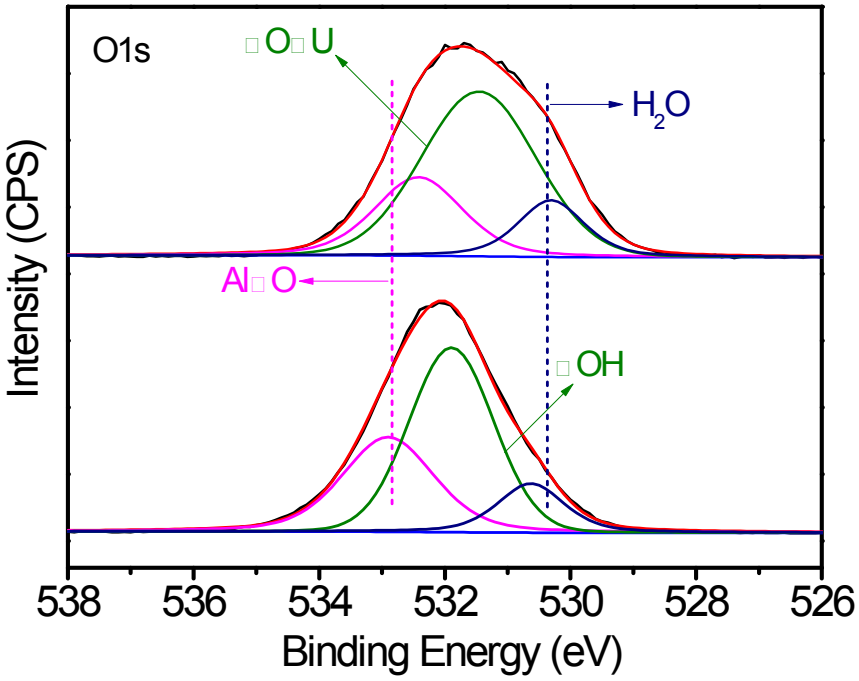

Figure S21. XPS high-resolution spectra of O1s for Al_2O_3-Cl before and after U(VI) adsorption.

References

[S1]M. Sprynskyy, T. Kowalkowski, H. Tutu, E. M. Cukrowska and B. Buszewski, Adsorption performance of talc for uranium removal from aqueous solution. Chemical Engineering Journal. 2011, 171, 1185-1193.

[S2]P. Singhal, B. G. Vats, A. Yadav and V. Pulhani, Efficient extraction of uranium from environmental samples using phosphoramide functionalized magnetic nanoparticles: Understanding adsorption and binding mechanisms. Journal of Hazardous Materials. 2019, DOI: 10.1016/j.jhazmat.2019.121353.

[S3]H. Li, Y. Li, B. Li, Y. Dai and Xi Chen, Melamine-induced novel MSONs heterostructured framework: Controlled-switching between MOF and SOF via a self-assembling approach for rapid uranium sequestration. Chemical Engineering Journal. 2020, DOI: 10.1016/j.cej.2019.122279.

[S4]J. Zhu, Q. Liu, Z. Li, J. Liu, H. Zhang, R. Li and J. Wang, Efficient extraction of uranium from aqueous solution using an amino-functionalized magnetic titanate nanotubes. Journal of Hazardous Materials. 2018, 353, 9-17.

[S5]Y. Li, L. Wang, B. Li, M. Zhang, R. Wen, X. Guo, X. Li, J. Zhang, S. Li and L. Ma, Pore-free matrix with cooperative chelating of hyperbranched ligands for high-performance separation of uranium. ACS Applied Materials & Interfaces. 2016, 8, 28853-28861.

[S6]S. Das, S. Brown, R.T. Mayes, C. J. Janke, C. Tsouris, L. J. Kuo, G. Gill, S. Dai, Novel Poly(imide dioxime) Sorbents: Development and Testing for Enhanced Extraction of Uranium from Natural Seawater. Chemical Engineering Journal. 2016, 298, 124-135.

[S7]D. Shao, X. Wang, X. Ren, S. Hu, J. Wen, Z. Tan, J. Xiong, A. M. Asiri and H. M. Marwani, Polyamidoxime functionalized with phosphate groups by plasma technique for effective U(VI) adsorption. Journal of Industrial and Engineering Chemistry. 2018, 67, 380-387.